EURASIP Journal on Advances in Signal Processing

RESEARCH Open Access

Time delay estimation method based on generalized logarithmic hyperbolic secant function in impulsive noise

Yuzi Dou, Omer M. Abdelrhman and Sen Li*

*Correspondence: listen@dlmu.edu.cn

College of Information Science and Technology, Dalian Maritime University, Dalian 116026, China

Abstract

In this paper, a generalized logarithmic hyperbolic secant (GLHS) function is introduced that can effectively suppress impulsive noise while guarding the signal of interest from damage. Also, an analysis of the optimal scaling parameter choices for the GLHS function was studied. Then, in order to address the performance drawbacks of the traditional time delay estimation methods based on correlation under an impulsive noise environment, a novel GLHS-based correlation (GLHSC) is further developed, and the reliable time delay estimation result is obtained by finding the peak of GLHSC. The comprehensive Monte Carlo simulation results demonstrate that the performance of the method based on GLHSC is better than other robust competitive methods based on correlation in terms of probability of resolution and estimation accuracy, especially in a heavy-tailed noise environment.

Keywords: α-stable distribution, Time delay estimation, Nonlinear preprocessing, Logarithmic hyperbolic secant function, Impulsive noise

1 Introduction

Time delay estimation (TDE) is a fundamental signal processing problem and has wide applications, such as radar [1], system and process control [2, 3], and wireless communications [4–7]. In the past decades, TDE methods have gained the attention of researchers and have been widely studied. These TDE methods are mainly based on second-order statistics (SOS) or higher-order statistics (HOS) and have been proven that they exhibit outstanding performances under the assumption of Gaussian distribution noise [8, 9].

However, for now, it has been demonstrated that the popular Gaussian approximation is not adequate for describing the actual noise, which exhibits impulsive behavior in many situations [10], such as sudden bursts or sharp spikes, atmospheric noise, and sea clutter. Professor Nikias proposed that α-stable distribution is more appropriate for describing this kind of impulsive noise [11], which has been recognized by scholars in various academic research fields. Unfortunately, the SOS of the α-stable distribution with characteristic exponent $0 < \alpha < 2$ is infinite, and thus, the performance of the conventional signal processing methods based on SOS is seriously degraded in

the α-stable distribution noise environment. Professor Nikias's team and the related researchers who continue to study this situation defined fractional lower-order statistics (FLOS), which can replace the SOS used in the conventional signal processing methods, including robust covariation (ROC) [12], fractional lower-order moment (FLOM) [13, 14], and phased fractional lower-order moment (PFLOM) [15]. In this context, the TDE methods based on FLOS were proposed and analyzed in [16–18]. Although the TDE methods based on FLOS are robust to impulsive noise, the fractional lower-order parameter of FLOS is determined by the characteristic exponent of α-stable distribution, which is difficult to estimate in practice.

Inspired by the principles of information-theory learning and kernel functions, Professor Principe's team defined a kind of statistics named correntropy [19]. By employing the correntropy, the adaptive filtering problem [20], the direction of arrival estimation problem [21], and the TDE problem [22] in impulsive noise scenarios have been addressed. In [23], a correntropy-based correlation (CRCO) was proposed and applied to estimate the direction of arrival in impulsive noise. As the Gaussian kernel function used in correntropy is a bounded function compared to the p-order moment transformation used in FLOS, it follows that correntropy has a better suppression effect on impulsive noise than FLOS. The most important thing for the signal processing methods based on correntropy is that the selection of kernel width has a weak reliance on the characteristic exponent of α-stable distribution noise, which is another important advantage over FLOS.

Another robust method that can suppress impulsive noise is nonlinear preprocessing. To eliminate outliers, the amplitude of the received signals containing impulsive noise is limited by using a nonlinear preprocessing function. The most frequently used nonlinear preprocessing function is the hyperbolic tangent (tanh) function. In [24], a robust energy detector based on the tanh function was proposed to solve the problem that the performance of spectrum sensing algorithm degrades under an impulsive noise environment. To preserve the information of the original signal, a hyperbolic tangent transform was defined in [25] by introducing a preset parameter into the tanh function, and the selection of the present parameter is closely related to the amplitude of the original signal. Then, the hyperbolic tangent transform-based correlation (HTC) was proposed to solve the TDE problem [26] and the joint time delay–Doppler shift estimation problem [27] in impulsive noise. Further, by combining the correntropy with the tanh-based correlation (TC) function [26], a robust generalized correlation (GC) was defined in [28] and applied to estimate the direction of arrival in impulsive noise.

In this paper, inspired by the use of a nonlinear preprocessing method to limit amplitude, firstly, we define a generalized logarithmic hyperbolic secant (GLHS) function and analyze the optimal selection of scaling parameters in the GLHS function. Next, a novel GLHS-based correlation (GLHSC) is further developed and utilized to estimate time delay to address the performance degradation of the conventional time delay estimation methods based on correlation under an impulsive noise environment. The comprehensive Monte Carlo simulation results demonstrate that the performance of the proposed method outperforms its counterparts, especially in a heavy-tailed noise environment.

The remainder of this paper is organized as follows. The α-stable distribution model is briefly reviewed in Sect. 2, In Sect. 3, a novel nonlinear preprocessing function named the GLHS function is defined and the proper range of the scaling parameter is discussed.

Then, the GLHSC is defined and applied to construct a robust TDE method. In Sect. 4, simulation results for the proposed method are provided and discussed. The conclusion is finally drawn in Sect. 5.

2 Noise model

Since the probability density function (PDF) of the α-stable distribution lacks a unified closed-form expression, it is commonly expressed by its characteristic function [11]

$$\varphi(t) = \exp\{j\mu t - \gamma|t|^{\alpha}[1 + j\beta \mathrm{sign}(t) w(t,\alpha)]\}, \tag{1}$$

where

$$w(t,\alpha) = \begin{cases} \tan(\pi\alpha/2) & \alpha \neq 1 \\ (2/\pi)\log|t| & \alpha = 1 \end{cases} \tag{2}$$

and

$$\mathrm{sign}(t) = \begin{cases} 1, & t > 0 \\ 0, & t = 0 \\ -1, & t < 0 \end{cases} \tag{3}$$

$$\alpha \in (0,2], \beta \in [-1,1], \gamma \in (0,+\infty), \mu \in (-\infty,+\infty), \tag{4}$$

where α denotes the characteristic exponent that controls the thickness of the tails of the PDF. Smaller α leads to a heavier tail, indicating that the noise is more impulsive. β represents the symmetry parameter, which can describe the slope of the distribution. γ is a dispersion parameter that is similar to the variance of the Gaussian distribution. μ is a location parameter, when $\alpha \in (0,1)$ or $\alpha \in [1,2]$, μ denotes the median or the mean, respectively. When $\beta = 0$, the α-stable distribution is symmetric about μ and is called symmetric α-stable ($S\alpha S$) distribution. For the $S\alpha S$ distribution, when $\alpha = 1$ or $\alpha = 2$, $S\alpha S$ distribution is equivalent to the Cauchy distribution or the Gaussian distribution, respectively.

3 Methods

3.1 Proposed GLHS function

In this section, we first define a novel nonlinear preprocessing function with an adjustable parameter. Then, in order to keep the useful information of the original signal unchanged and reduce the effect of the impulsive noise, the optimal selection of the adjustable parameter is further discussed.

3.1.1 Definition

Inspired by the idea of amplitude limitation of the nonlinear preprocessing method, a generalized logarithmic hyperbolic secant (GLHS) function is defined.

Definition 1 GLHS function of a random variable s is defined as

$$f_{\mathrm{GLHS}}(x) = \frac{-\ln \operatorname{sech}(\lambda s)}{\lambda s}, \tag{5}$$

where $\lambda > 0$ is a scaling parameter. $\ln(\bullet)$ is a natural logarithm, $\operatorname{sech}(\bullet)$ is a hyperbolic secant function, and $\operatorname{sech}(s) = 2/(e^s + e^{-s})$. The curves of the GLHS function with different scaling parameters λ are shown in Fig. 1.

It is observed that the GLHS function is odd symmetric corresponding to the origin, and GLHS function increases monotonically as the $|s|$ increases. The curve of the GLHS function can be divided into two parts, i.e., an approximate linear area (ALA) part near zero point and a suppression area (SA) part far from zero point. In the SA part, no matter how large the amplitude of the variable s is, the output value tends to be ± 1 after the GLHS function preprocessing, so it plays an important role in suppressing the impulsive noise with large amplitude. In the ALA part, the GLHS function can be approximated as a linear function, so it can effectively maintain the useful information of the original signal unchanged. However, for the GLHS function with different scaling parameters λ, the corresponding range of the ALA part is different, and the degree of linear approximation of the ALA part is also different.

3.1.2 Scaling parameter selection of GLHS function

The more linear the ALA part is, the less influence on the useful information of the original signal the GLHS function will have. The most important factor affecting the degree of linear approximation of the ALA part is the scaling parameter λ, and thus, the selection of the proper scaling parameter is a problem worth discussing.

To analyze the degree of linear approximation of the GLHS function located in the ALA part, the range of the ALA part needs to be measured. Since curvature represents the degree to which a curve deviates from a straight line, the signal value corresponding to the maximum curvature point (defined as s_{zone}) is selected as the

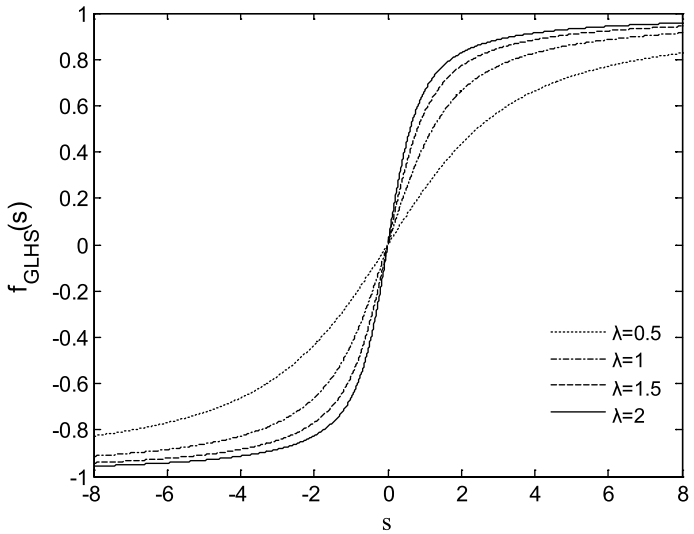

Fig. 1 The GLHS function curves with different scaling parameters

Table 1 The different s_{zone} corresponding to the different scaling parameters of GLHS function

λ	**0.1**	**0.2**	**0.3**	**0.4**	**0.5**	**0.6**	**0.7**
s_{zone}	8.48	4.25	2.85	2.16	1.73	1.48	1.29
λ	0.8	0.9	1.0	1.2	1.4	1.6	1.8
s_{zone}	1.15	1.04	0.95	0.83	0.75	0.68	0.64
λ	2.0	2.2	2.4	2.6	2.8	3.0	3.2
s_{zone}	0.60	0.57	0.54	0.52	0.50	0.49	0.47
λ	3.4	3.6	3.8	4.0	4.2	4.6	4.8
s_{zone}	0.46	0.45	0.44	0.42	0.41	0.41	0.40
λ	5.0	5.2	5.4	5.6	5.8	6.0	6.2
s_{zone}	0.38	0.37	0.37	0.36	0.35	0.35	0.34

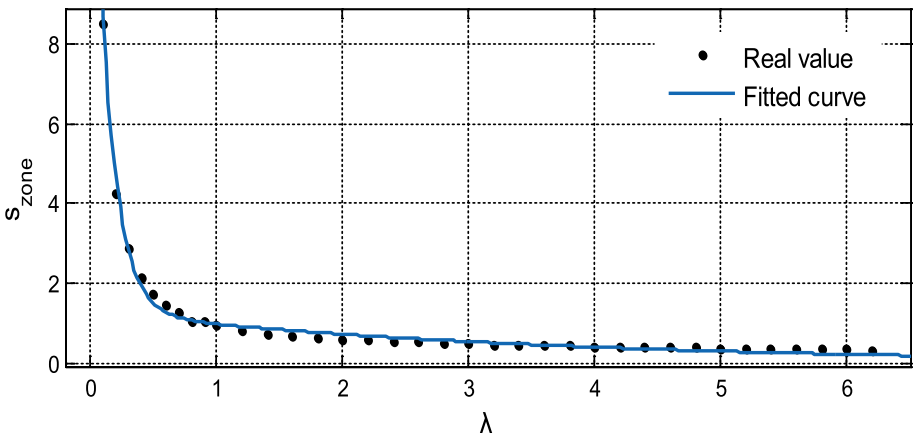

Fig. 2 s_{zone} corresponding to λ and its fitted curve

maximum range of the ALA part. In other words, s_{zone} is a dividing point between the ALA part and the SA part, and the range of the ALA part is $[-s_{\text{zone}}, s_{\text{zone}}]$.

Due to different s_{zone} generated by different scaling parameters λ, Table 1 shows the relationship between s_{zone} and λ.

The data in Table 1 are fitted by a second-order exponential function. According to Table 1, the formula of the fitted curve is shown in Eq. (6), and the fitted figure is shown in Fig. 2.

$$s_{\text{zone}} = 14.7\exp(-7.28\lambda) + 1.3\exp(-0.3\lambda). \tag{6}$$

It can be seen from Fig. 2 that when $\lambda \in (0, 1)$, the range of the ALA part of the GLHS function changes a lot. When $\lambda \in (1, +\infty)$, the range of the ALA part of the GLHS function changes little. Thus, in the following demonstration, we select the spacing of the scaling parameters λ in the range $\lambda \in (0, 1)$ to be 0.1 and the spacing in the range $\lambda \in (1, +\infty)$ to be 0.5.

In the ALA part, as it can be approximated as a linear function with a slope of k passing through the origin point, the GLHS function can effectively maintain the useful information of the original signal unchanged. For the GLHS functions with

different scaling parameters λ, the slope k of the corresponding linear function is different, and the degree of approximation between the GLHS function and the linear function is also different. It can be considered that the better the approximation between the GLHS function and the linear function, the stronger the ability of the GLHS function to maintain the useful information of the original signal unchanged. Three indicators are used to measure the degree of approximation between the GLHS function and the linear function, i.e., squares due to error (SSE), root mean square error (RMSE), and R-square, which are defined as.

$$\mathrm{SSE} = \sum_{l=1}^{L} \left(y_l - \widehat{y_i}\right)^2, \tag{7}$$

$$\mathrm{RMSE} = \sqrt{\frac{1}{L}\sum_{l=1}^{L} \left(y_l - \widehat{y_i}\right)^2}, \tag{8}$$

$$\text{R - square} = \frac{\sum_{l=1}^{L} \left(\widehat{y_i} - y_l\right)^2}{\sum_{l=1}^{L} \left(y_l - \overline{y_i}\right)^2}, \tag{9}$$

where $y_l = f_{\mathrm{GLHS}}(s_l)$, $\widehat{y_i} = ks_l$ is the linear function, $\overline{y_i}$ is the mean of y_l, and $s_l, l = 1, 2, \cdots L$ is the uniform sampling value in the range $[-s_{zone}, s_{zone}]$. The closer SSE and RMSE are to 0, and the closer R-square is to 1, which means that the better the degree of approximation between the GLHS function and the linear function. The slope k and the degree of linear approximation of the GLHS functions with different scaling parameters λ are given in Table 2.

As shown in Table 2, from the perspective of the RMSE and the R-square indicators, the smaller the scaling parameter λ, the better the degree of linear approximation of the GLHS function. However, from the perspective of the SSE indicator, the variation rule of the degree of linear approximation of the GLHS function with scaling parameter λ is different in the range where $\lambda > 1$ and $\lambda < 1$. In addition, it can be seen from Table 1 that when the scaling parameter λ is relatively small, the ALA part is relatively large (the SA part is relatively small at the same time), which is not conducive to suppressing the impulsive noise. However, when the scaling parameter λ is relatively large, the ALA part is relatively small (the SA part is relatively large at the same time), which is not conducive to keeping the useful information of the signal unchanged. Therefore, to summarize these effects, in order to obtain both a better degree of linear approximation of the GLHS function located in the ALA part and a better effect for suppressing impulsive noise, the scaling parameter λ is selected in the range $\lambda \in [0.2, 1]$.

3.2 Application on TDE

3.2.1 Signal model

In the problem of TDE, two received signals $x(t)$and$g(t)$ are defined as.

$$x(t) = s(t) + n_1(t), \tag{10}$$

Table 2 The slope k and the degree of linear approximation of the GLHS functions with different scaling parameters λ

λ	k	SSE	RMSE	R-square
0.1	0.0468	0.3371	0.0063	0.9968
0.2	0.0935	0.1732	0.0064	0.9967
0.3	0.1402	0.1207	0.0065	0.9966
0.4	0.1868	0.0962	0.0067	0.9965
0.5	0.2331	0.0830	0.0068	0.9964
0.6	0.2792	0.0757	0.0071	0.9962
0.7	0.3250	0.0718	0.0074	0.9959
0.8	0.3706	0.0703	0.0078	0.9957
0.9	0.4157	0.0708	0.0082	0.9953
1	0.4605	0.0723	0.0086	0.9950
1.5	0.6780	0.0975	0.0116	0.9898
2	0.8841	0.1451	0.0155	0.9887
2.5	1.0790	0.2141	0.0199	0.9838
3	1.2630	0.2976	0.0245	0.9780
3.5	1.4400	0.3914	0.0292	0.9717
4	1.6090	0.4926	0.0338	0.9648
4.5	1.7720	0.5999	0.0384	0.9575
5	1.9310	0.6974	0.0425	0.9504

$$g(t) = s(t - D) + n_2(t), \tag{11}$$

where D is the time delay between two received signals. n_1(t) and n_2(t) denote the additive noises, which are uncorrelated with each other and are independent of the signal s(t). The conventional TDE methods using second-order statistics (SOS) are easy to implement and have a satisfactory estimation performance in the Gaussian noise environment. However, when the additive noise deviates from the ideal Gaussian distribution and is characterized by the $S\alpha S$ distribution, SOS of $S\alpha S$ distribution noise with characteristic exponent $\alpha \in (0, 2)$ is infinite, resulting in the severe degradation of performance of TDE methods based on SOS in the $S\alpha S$ distribution noise environment.

3.2.2 Proposed GLHSC-based TDE method

In this section, GLHS-based correlation (GLHSC) is defined and applied to solve the TDE problem in the $S\alpha S$ distribution noise environment.

GLHSC of two signals $x(t)$and$g(t)$ is defined as

$$R^{xg}_{\mathrm{GLHSC}}(\tau) = E\left[f_{\mathrm{GLHS}}(x(t))\left(f_{\mathrm{GLHS}}\left(g(t+\tau)\right)\right)^*\right], \tag{12}$$

where $E[\bullet]$ indicates the statistical expectation operator, and $(\bullet)^*$ is the conjugate operator. $R^{xg}_{\mathrm{GLHSC}}(\tau)$ can be regarded as the correlation of two signals $x(t)$and$g(t)$ after nonlinear preprocessing by GLHS function. According to the analysis of the GLHS function, the impulsive noise embedded in the received signal is usually located in the SA part due to the large amplitude of the impulsive noise, and thus, GLHS function can play a good inhibitory effect by limiting the amplitude of the impulsive noise. However, the signal $s(t)$ in the received signal is usually located in the ALA part, in which the GLHS

function is an approximately linear function that is conducive to maintaining the characteristics of the signal itself unchanged. Therefore, $R^{xg}_{GLHSC}(\tau)$ has the maximum value when $\tau = D$, and the time delay can be estimated by searching the peak of $R^{xy}_{GLHSC}(\tau)$,

$$\hat{D} = \text{argmax}\left|R^{xg}_{\text{GLHSC}}(\tau)\right|. \tag{13}$$

4 Results and discussion

Consider the case that the received signals $x(t)$and$g(t)$ are quadrature amplitude modulated (QAM) signals and the additive noise is modeled by the $S\alpha S$ distribution model with the characteristic exponent α. The variance of $S\alpha S$ distribution is infinite, and thus, the conventional signal-to-noise ratio (SNR) is no longer effective. In this context, the concept of generalized signal-to-noise ratio (GSNR) is defined as the ratio between the signal power and the noise dispersion γ as follows

$$\text{GSNR} = 10\log_{10}\left(\frac{|s(t)|^2}{\gamma}\right). \tag{14}$$

In this section, by comparing the performances of the GHLSC-based TDE methods with different scaling parameters λ, we verify the results of the optimal selection of scaling parameter discussed in Sect. 3.1.2. In addition, a battery of numerical simulations is conducted to compare the performance of the proposed GHLSC-based TDE method with existing TDE estimation methods, including ROC-based TDE method, FLOC-based TDE method, PFLOC-based TDE method, CRCO-based TDE method, TC-based TDE method, HTC-based TDE method, and GC-based TDE method. The performance indicator named RMSE for the TDE method is calculated by.

$$\text{RMSE} = \sqrt{\frac{1}{M}\sum_{m=1}^{M}\left|\hat{d}_m - D\right|^2}. \tag{15}$$

Another performance indicator named probability of resolution P_{a} is calculated by

$$P_{\text{a}} = \left(1 - \frac{1}{M}\sum_{m=1}^{M}\frac{\left|\hat{d}_m - D\right|}{D}\right) \times 100\%. \tag{16}$$

where $\widehat{d}_m$ is the mth estimated value of the true time delay D, and $D = 20$ sample interval is used in simulation experiments. Besides a single estimation experiment, each simulation experiment will be executed for $M = 500$ independent Monte Carlo experiments.

4.1 Selection of scaling parameters λ

To verify the influence of the scaling parameters λ on the performance of the GLHSC-based TDE method in the $S\alpha S$ distribution noise environment, the characteristic exponent of $S\alpha S$ distribution is set from strong impulsiveness $\alpha = 1$ to weak impulsiveness $\alpha = 2$, and the cases of GSNR = 2dB are given, and the estimation performances of the GLHSC-based TDE methods with different scaling parameters λ are shown in Fig. 3.

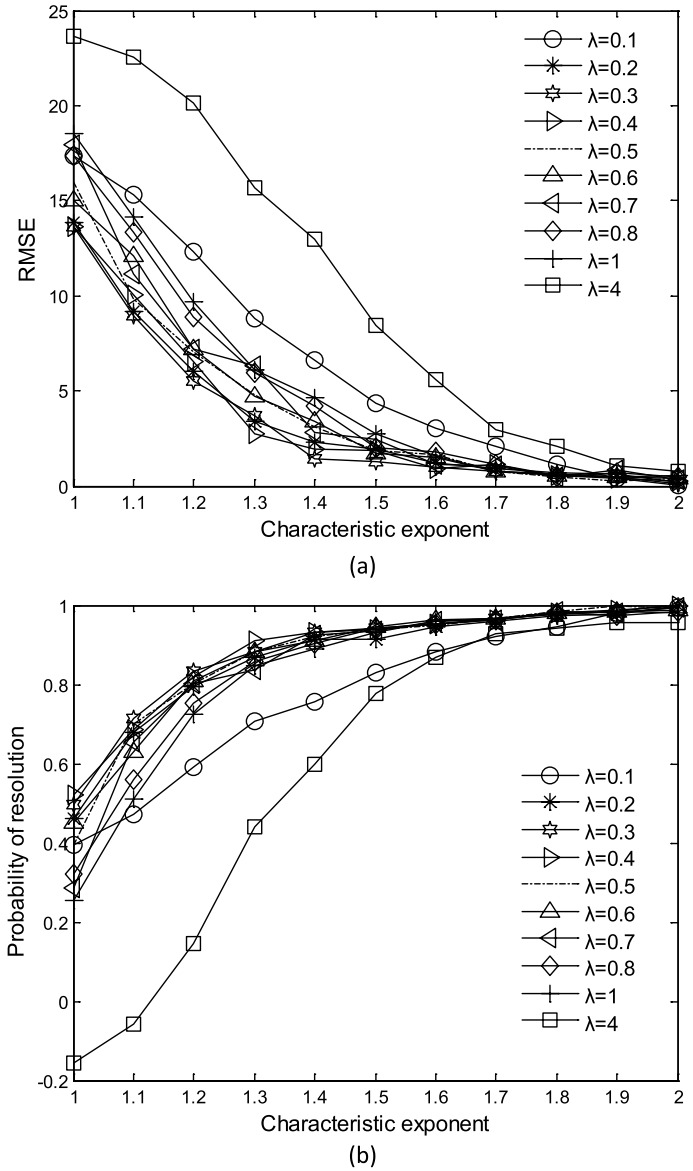

Fig. 3 Performances of the GLHSC-based TDE methods with different scaling parameters λ (GSNR = 2dB) **a** RMSE, **b** Probability of resolution

It can be seen from Fig. 3 that when the scaling parameter is a fixed constant, as the increase in the characteristic exponent, the RMSEs of the proposed methods decrease, and the probabilities of resolution of the proposed methods improve. When the scaling parameter λ is greater than 1, the ALA part of the GLHS function is relatively small, so it is not conducive to keeping the useful information of signals. Simultaneously, the GLHSC-based TDE methods perform poorly since the degree of linear approximation of the GLHS function located in the ALA part is not good. When the scaling parameter λ is less than 0.2, the degree of linear approximation of the GLHS function located in the ALA part is good, but the range of the ALA part is relatively large at the same time. It is not conducive to inhibiting the impulsive noise, and thus, it follows that the performance of the GLHSC-based TDE method is also not good. When the scaling parameter

$0.2 \leq \lambda \leq 1$, the GLHSC-based TDE methods have a good estimation performance, because the ranges of the SA and the ALA parts are reasonable and there is a good linear approximation in the ALA part. $\lambda = 0.3$ is selected for the GLHSC-based TDE method in the following simulation experiments.

4.2 A single estimate experiment

To directly reflect the effectiveness of the proposed method for estimating time delay in the $S\alpha S$ distribution noise, GSNR = 0dB and the characteristic exponent $\alpha = 1.4$ are used, and a single estimation result of the eight methods is shown in Fig. 4.

As can be seen from Fig. 4, compared with the other seven methods which are based on FLOS, correntropy, and tanh function, the GLHSC-based TDE method has the sharpest peak value, and the difference between the peak value and the secondary peak value is the largest, so it is most conducive to accurately estimating correct time delay.

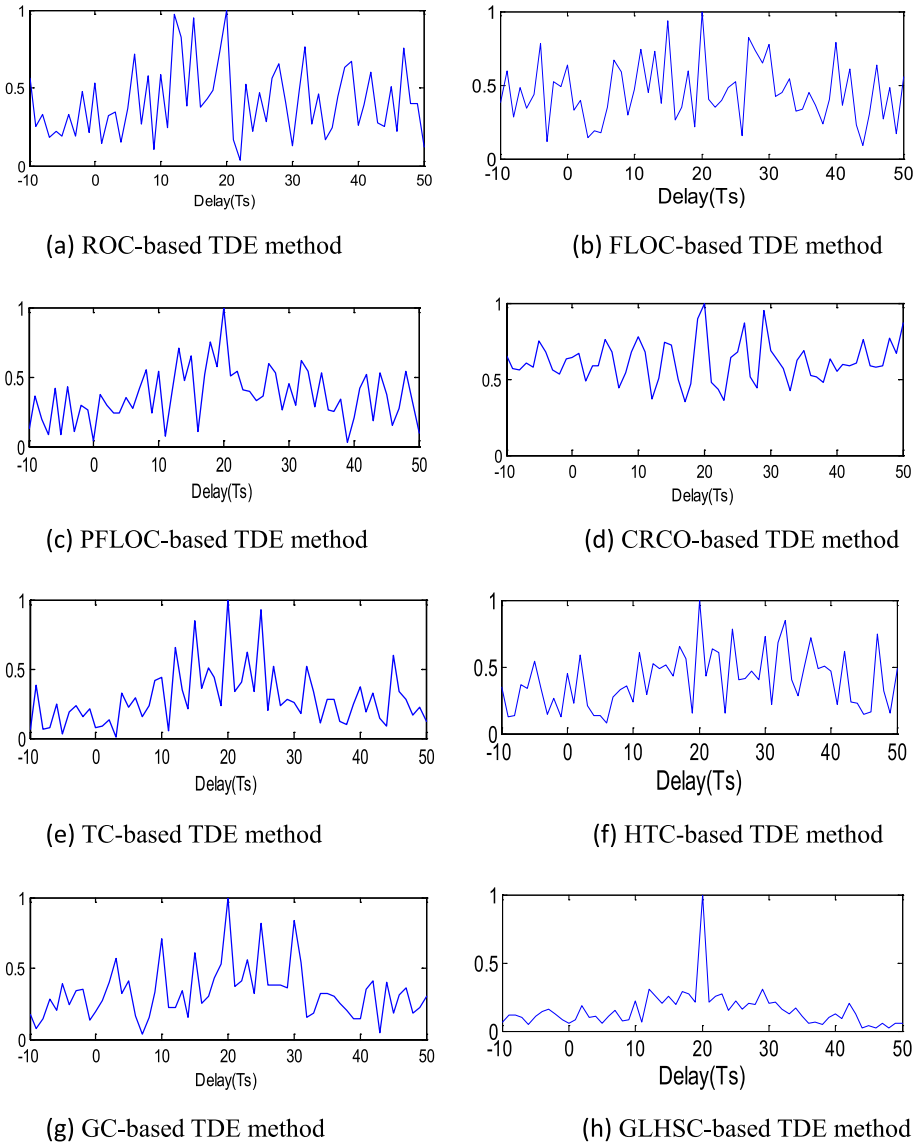

Fig. 4 The single estimation results of the eight methods in $S\alpha S$ distribution noise (GSNR = 0dB and $\alpha = 1.4$)

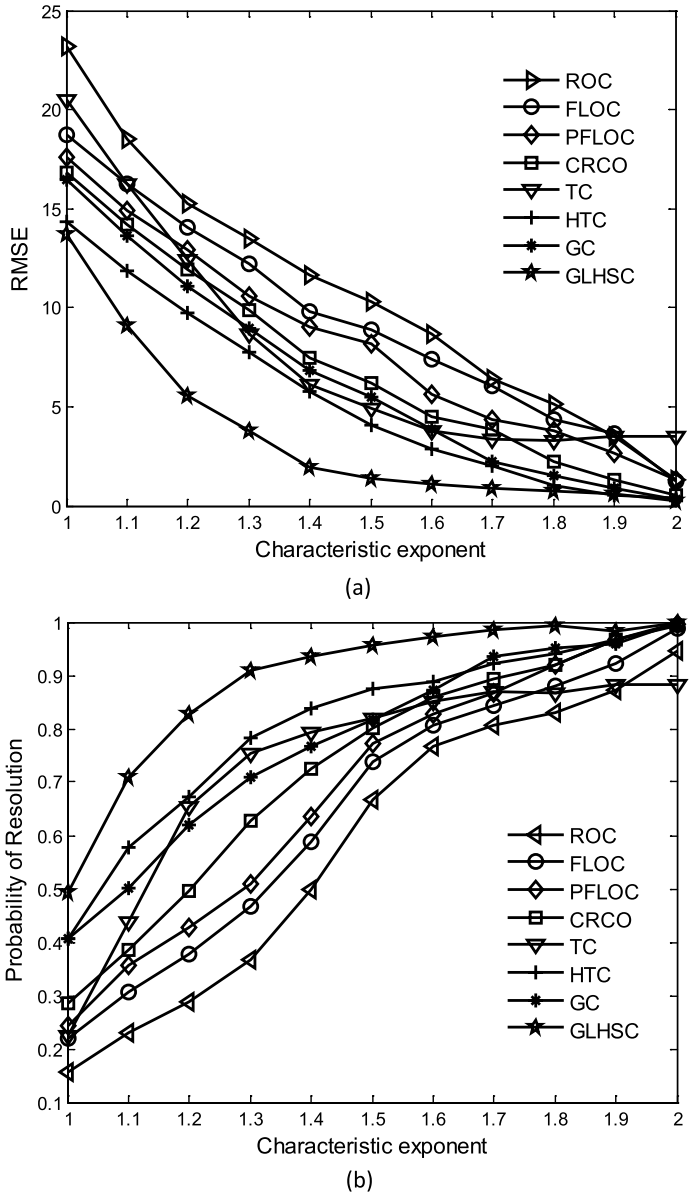

Fig. 5 Performance versus characteristic exponent (GSNR = 2dB). **a** RMSE, **b** Probability of resolution

4.3 Monte Carlo experiments

Experiment 1: Simulations with different characteristic exponents. To verify the robustness of the proposed method to impulsive noise, GSNR = 2dB is used, and the characteristic exponent of $S\alpha S$ distribution is set from strong impulsiveness $\alpha = 1$ to weak impulsiveness $\alpha = 2$. The performances of the eight methods are shown in Fig. 5.

It can be seen that as the increase in characteristic exponent α, the RMSEs of the eight methods decrease and the probabilities of resolution of the eight methods increase. Note that the performances of all methods are similar in the environment close to Gaussian noise $\alpha = 2$. However, the performance of the GHLSC-based TDE method is better than the competitors under the $1 < \alpha < 1.8$ strong impulsiveness environments. For example, when $\alpha = 1.2$, the probability of resolution of the GHLSC-based TDE method can reach

83%, the probabilities of resolution of the HTC and TC-based TDE methods are 67% and 65%, respectively, and the probability of resolution of the GC-based TDE method is 62%, whereas the probabilities of resolution of the CRCO, PFLOC, FLOC, and ROC-based TDE methods are less than 50%.

Experiment 2: Simulations with different GSNRs. Considering the cases of $S\alpha S$ distribution noise with characteristic exponent $\alpha = 1.2$. When the GSNR ranges from $-$ 2dB to 10 dB, the performances of the eight methods are shown in Fig. 6.

It can be seen that as the GSNR increases, the RMSEs of the eight methods decrease, and the probabilities of resolution of the eight methods increase. However, the performance of the GHLSC-based TDE method is better than that of the other seven methods. For example, when GSNR $=$ 6dB, the probability of resolution of the

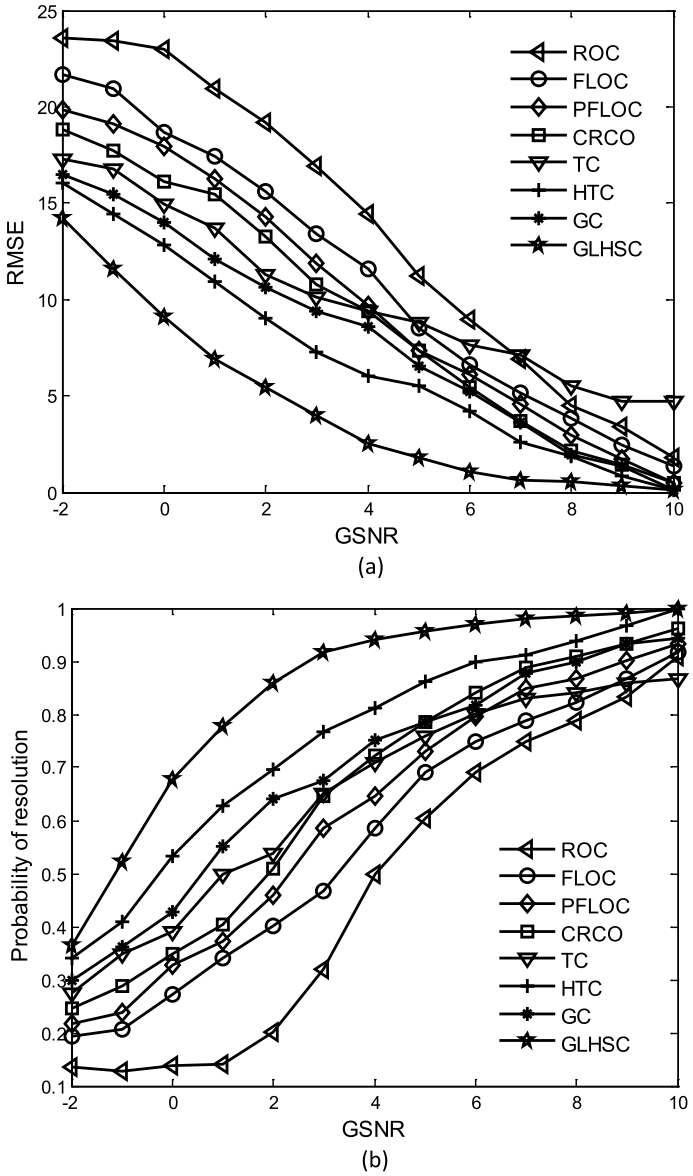

Fig. 6 Performance versus GSNR ($\alpha = 1.2$). **a** RMSE, **b** Probability of resolution

GHLSC-based TDE method can reach 95%, and the probability of resolution of the HTC-based TDE method is 86%, whereas the probabilities of resolution of the other six methods are less than 80%.

5 Conclusion

In this paper, a novel TDE method is proposed in order to contend with the problem that the TDE methods based on conventional correlation degrade under an impulsive noise environment. First, the GLHS preprocessing function is defined which can keep the useful information of signal sources unchanged and limit the amplitude of the impulsive noise within the bounds, and then, the optimal selection of the scaling parameter regarding the GLHS function is discussed. Subsequently, GLHSC is constructed and used to estimate time delay in impulsive noise. The reliable estimation result is obtained by finding the peak of the GLHSC. The simulations demonstrate the superiority of the proposed method compared to the existing methods, especially in the environment of heavy-tailed noise.

Abbreviations

TDE	Time delay estimation
GLHS	Generalized logarithmic hyperbolic secant
GLHSC	Generalized logarithmic hyperbolic secant-based correlation
SOS	Second-order statistics
HOS	Higher-order statistics
FLOS	Fractional lower-order statistics
ROC	Robust covariation
FLOC	Fractional lower-order correlation
PFLOC	Phased fractional lower-order statistics
CRCO	Correntropy-based correlation
HTC	Hyperbolic tangent transform-based correlation
GC	Generalized correlation
PDF	Probability density function
$S\alpha S$	Symmetric α-stable
ALA	Approximate linear area
SA	Suppression area
SSE	Squares due to error
RMSE	Root mean square error
SNR	Signal-to-noise ratio
GSNR	Generalized signal-to-noise ratio

Acknowledgements

The authors would like to thank anyone who supported the publication of this paper.

Author contributions

YD and SL contributed to the research idea, methods, and simulations and drafted the manuscript. OM further examined the manuscript. All authors read and approved the final manuscript.

Funding

This work was supported in part by the National Natural Science Foundation of China under Grant (61971083) and in part by the fundamental research funds for the central university under Grants (3132019341).

Availability of data and materials

Data sharing is not applicable to this article as no datasets were generated or analyzed during the current study.

Declarations

Competing interests

The authors declare that they have no competing interests.

Received: 15 July 2022 Accepted: 10 November 2022
Published online: 26 November 2022

References

1. J. Pan, M. Sun, Y. Wang, C. Le Bastard, V. Baltazart, Time-delay estimation by a modified orthogonal matching pursuit method for rough pavement. IEEE Trans. Geosci. Remote Sensing. **59**(4), 2973–2981 (2021)
2. Y. Wang, M. Leibold, J. Lee, W. Ye, J. Xie, and M. Buss, Incremental model predictive control exploiting time-delay estimation for a robot manipulator. IEEE Trans. Control Syst. Technol. To be published. https://doi.org/10.1109/TCST.2022.3142629.
3. F. Kocak, H. Celebi, S. Hasari, S. Gezici, K. Qaraqe, H. Aralan, and H. V. Poor, Time-delay estimation in dispersed spectrum cognitive radio systems. EURASIP J. Adv. Signal Process. (2010).
4. X. Li and X. Ma, Joint doppler shift and time delay estimation by deconvolution of generalized matched filter. EURASIP J. Adv. Signal Process. (2021).
5. H. Xu, F. Ding, B. Champagne, Joint parameter and time-delay estimation for a class of nonlinear time-series models. IEEE Signal Process. Lett. **29**, 947–951 (2022). https://doi.org/10.1109/LSP.2022.3152108
6. T. Jagadesh, B. Sheela Rani, Time delay estimation in radar system using fuzzy based iterative unscented Kalman filter. Comput. Syst. Sci. Eng. **44**(3), 2569–2583 (2022)
7. Y. Guo, Z. Liu, Time-delay-estimation-liked detection algorithm for LoRa signals over multipath channels. IEEE Wirel. Commun. Lett. **9**, 1093–1096 (2020)
8. G.B. Giannakis, M.K. Tsatsanis, Signal detection and classification using matched filtering and higher order statistics. IEEE Trans. Acoust. Speech Signal Process. **38**(7), 1284–1296 (1990)
9. J.R. Fonoliosa, C.T. Nikias, Wigner higher order moment spectra: definition, properties, computation and application to transient signal analysis. IEEE Trans. Signal Process. **41**(1), 245–266 (1993)
10. L. Gao, X. Li, D. Bi, L. Peng, X. Xie, Y. Xie, Robust tensor recovery in impulsive noise based on correntropy and hybrid tensor sparsity. IEEE Trans. Circuits Syst. II-Express Briefsss **69**(3), 1857–1861 (2022)
11. C.L. Nikias, M. Shao, *Signal processing with alpha-stable distributions and applications* (Wiley, New York, 1995)
12. P. Tsakalides, C.L. Nikias, The robust covariation-based MUSIC (ROC-MUSIC) algorithm for bearing estimation in impulsive noise environments. IEEE Trans. Signal Process. **44**(7), 1623–1633 (1996)
13. X. Ma, C.L. Nikias, Joint estimation of time delay and frequency delay in impulsive noise using fractional lower order statistics. IEEE Trans. Signal Process. **44**(11), 2669–2687 (1996)
14. G.A. Tsihrintzis, C.L. Nikias, Evaluation of fractional lower-order statistics-based detection algorithms on real radar sea-clutter data. IET Radar Sonar Navig. **144**(1), 29–37 (1997)
15. H. Belkacemi, Sylvie marcos, robust subspace-based algorithms for joint angle-doppler estimation in non-gaussian clutter. Signal Process. **87**(7), 1547–1558 (2007)
16. P.G. Georgiou, P. Tsakalides, C. Kyriakakis, Alpha-stable modeling of noise and robust time-delay estimation in the presence of impulsive noise. IEEE Trans. Multimedia **1**(3), 291–301 (1999)
17. W. Zeng, H.C. So, A.M. Zoubir, An *lp*-norm minimization approach to time delay estimation in impulsive noise. Digit. Signal Prog. **23**(4), 1247–1254 (2013)
18. B. Satar, G. Soysal, X. Jiang, M. Efe, T. Kirubarajan, Robust weighted *l*(1,2) norm filtering in passive radar systems. Sensors **20**(11), 1824–1832 (2020)
19. W. Liu, P.P. Pokharel, J.C. Principe, Correntropy: properties and applications in non-gaussian signal processing. IEEE Trans. Signal Process. **55**(11), 5286–5298 (2007)
20. B. Chen, Y. Xie, Z. Li, Y. Li, P. Ren, Asymmetric correntropy for robust adaptive filtering. IEEE Trans. Circuits Syst. II-Express Briefs. **69**(3), 1922–1926 (2022)
21. Y. Dou, S. Li, Kernel function-based ambiguity function and its application on DOA estimation in impulsive noise. Sensors **22**(18), 6996 (2022). https://doi.org/10.3390/s22186996
22. F. Jin, T. Qiu, Adaptive time delay estimation based on the maximum correntropy criterion. Digit. Signal Prog. **88**, 23–32 (2019)
23. J.F. Zhang, T.S. Qiu, A.M. Song, H. Tang, A novel correntropy-based DOA estimation algorithm in impulsive noise environments. Signal Process. **104**, 346–357 (2014)
24. H. Qu, X. Xu, J. Zhao, F. Yan, W. Wang, A Robust hyperbolic tangent-based energy detector with gaussian and non-gaussian noise environments in cognitive radio system. IEEE Syst. J. **14**(3), 3161–3172 (2020)
25. T. Liu, T.S. Qiu, S.Y. Luan, Hyperbolic-tangent-function-based cyclic correlation: definition and theory. Signal Process. **164**, 206–216 (2019)
26. T. Liu, J.C. Zhang, S.Y. Luan, and T.S Qiu, Robust time delay estimation with unknown cyclic frequency in co-channel interference and impulsive noise. Digit. Signal Prog. 117, (2021). To be published. https://doi.org/10.1016/j.dsp.2021.103166
27. T. Liu, T.S Qiu, J.C. Zhang, and S.Y. Luan, Hyperbolic tangent cyclic correlation and its application to the joint estimation of time delay and doppler shift. Signal Process. 117, (2021). To be published. https://doi.org/10.1016/j.dsp.2021.103166.
28. S.Y. Luan, M.L. Zhao, Y.R. Gao, Z.J. Zhang, and T.S. Qiu, Generalized covariance for non-Gaussian signal processing and GC-MUSIC under Alpha-stable distributed noise. Digit. Signal Prog. 110,(2021), to be published. https://doi.org/10.1016/j.dsp.2021.103166.

Publisher's Note